

Fluorescence-Encoded Infrared Vibrational Spectroscopy with Single-Molecule Sensitivity

Lukas Whaley-Mayda, Abhirup Guha, Samuel B. Penwell, and Andrei Tokmakoff*



Cite This: *J. Am. Chem. Soc.* 2021, 143, 3060–3064



Read Online

ACCESS |



Metrics & More



Article Recommendations



Supporting Information

ABSTRACT: Single-molecule methods have revolutionized molecular science, but techniques possessing the structural sensitivity required for chemical problems—e.g. vibrational spectroscopy—remain difficult to apply in solution. Here, we describe how coupling infrared-vibrational absorption to a fluorescent electronic transition (fluorescence-encoded infrared (FEIR) spectroscopy) can achieve single-molecule sensitivity in solution with conventional far-field optics. Using the fluorophore Coumarin 6, we illustrate the principles by which FEIR spectroscopy measures vibrational spectra and relaxation and introduce FEIR correlation spectroscopy, a vibrational analogue of fluorescence correlation spectroscopy, to demonstrate single-molecule sensitivity. With further improvements, FEIR spectroscopy could become a powerful tool for single-molecule vibrational investigations in the solution or condensed phase.

Single-molecule (SM) spectroscopy has had a profound impact on how we describe molecular phenomena in chemistry, biology, and materials science. Studying the behavior of individuals reveals information hidden within the ensemble average, while the ability to access trajectories of a molecular observable at equilibrium provides dynamical information without the need for synchronization. Since the early pioneering experiments, fluorescence has become the most widely adapted method for SM detection, due to the bright, background-free signal coupled with sensitive single-photon detectors and modern microscopy tools.^{1–5} While the capabilities of SM fluorescence have been revolutionary, its limited structural specificity often restricts its applicability for chemical problems. This shortcoming has inspired a concurrent development of SM vibrational techniques, which offer a sensitivity to chemical bonding and specific molecular contacts through the frequencies and line shapes of vibrational bands. However, most of these methods, including surface- and tip-enhanced Raman spectroscopy (SERS and TERS),^{6–9} atomic force microscopy infrared spectroscopy (AFM-IR),¹⁰ infrared scattering-type scanning near-field optical microscopy (IR-sSNOM),¹¹ and scanning tunneling microscopy (STM),¹² require contact with a solid interface, probe, or nanostructure, precluding their application to solution-phase systems. This Communication presents evidence that infrared (IR) spectroscopy is possible with SM sensitivity using fluorescence encoding, providing a new strategy for SM vibrational spectroscopy compatible with chemical systems in solution.

Coupling the vibrational excitation to a fluorescent electronic transition is an attractive strategy that benefits from the experimental and technical advantages of far-field fluorescence detection, including solution-phase compatibility. Double resonance schemes that first excite vibrations via infrared absorption or stimulated Raman pumping and then up-convert the molecule to an emissive electronic excited state have existed since the 1970s to perform vibrational spectroscopy with increased detection sensitivity.^{13–18}

Recently, Xiong et al. achieved SM detection with stimulated Raman excited fluorescence (SREF) spectroscopy, representing the first far-field SM vibrational measurement.¹⁹ Our group has adapted an IR-pumped double resonance method, fluorescence-encoded IR (FEIR) spectroscopy, using broad-band femtosecond pulses to perform ultrafast Fourier transform vibrational spectroscopy,^{20,21} and recently developed a high-sensitivity experimental configuration incorporating confocal fluorescence microscopy to achieve 10–100 nM sensitivity in solution.²² Here we build on those results to perform FEIR correlation spectroscopy, an IR-vibrational analogue of fluorescence correlation spectroscopy (FCS), demonstrating that FEIR spectroscopy can achieve SM sensitivity, i.e. where on average less than one molecule contributes to the signal at any given time.

FEIR spectroscopy operates by the double resonance scheme depicted in Figure 1a. An IR pulse or pulse pair resonantly drives vibrations into their first excited state, after which an electronically preresonant visible pulse selectively brings the fluorophore to its electronic excited state. The resulting fluorescence emission intensity is therefore dependent on the excited vibrational population created by the IR field on the ground electronic state and is used as an action signal that encodes vibrational information. In practice, the weak IR-vibrational absorption cross sections and picosecond lifetimes necessitate intense pulses with comparable or shorter durations to ensure the overall excitation process is competitive against relaxation. Furthermore, high repetition

Received: January 15, 2021

Published: February 17, 2021



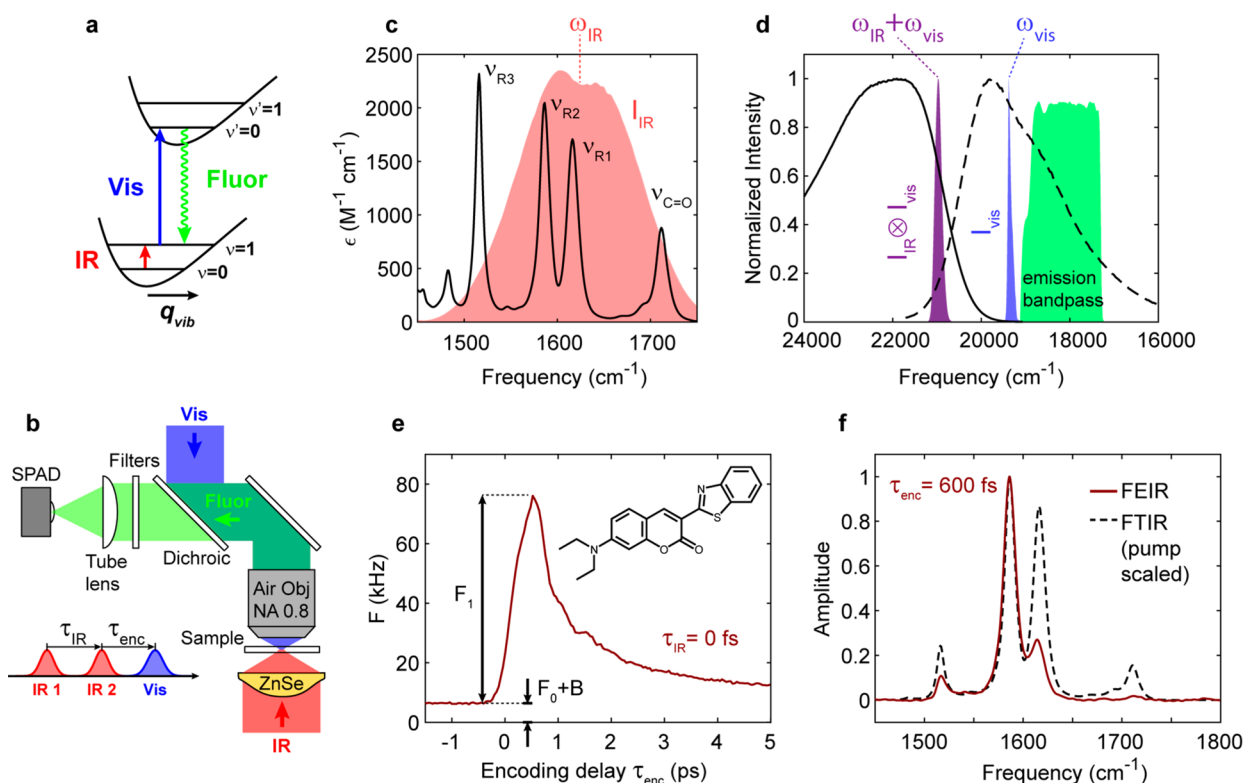


Figure 1. (a) Energy level diagram for FEIR spectroscopy. (b) Experimental schematic of the FEIR microscope and pulse sequence. (c) FTIR spectrum of C6 in acetonitrile- d_3 with IR pulse spectrum. (d) Electronic absorption (solid) and fluorescence (dashed) spectra with the visible pulse spectrum, convolution of visible and IR pulse spectra (distribution of their frequency sums), and emission bandpass. (e) 1-IR-pulse FEIR data on a $30 \mu\text{M}$ C6 solution. Molecular structure of C6 is inset. (f) FEIR spectrum of the same sample at $\tau_{\text{enc}} = 600 \text{ fs}$ compared with the FTIR spectrum scaled by the IR pulse spectrum. Data acquisition times for (e) and (f) were $< 5 \text{ min}$.

rates benefit single-photon counting but must be balanced with the technical requirements of generating intense, ultrashort mid-IR pulses and potential heating artifacts.

FEIR measurements are performed with the experimental scheme summarized in Figure 1b.²² We use 200–300 fs mid-IR and visible pulses derived from a 1 MHz fiber laser,²³ enabling time-resolved measurements of vibrational relaxation processes, as well as broad-band excitation of multiple modes. To achieve intense excitation fields and a small probe volume, the IR and visible beams are focused into the sample with high numerical aperture (NA) optics in a counter-propagating geometry, with the smaller diffraction-limited visible focus ($340 \text{ nm } 1/e^2$ radius, 0.2–30 pJ pulse energy) centered within the larger IR focus ($9 \mu\text{m}$, 50 nJ). Fluorescence is collected with the same visible objective lens, passed through selective bandpass filters, and imaged onto a single-photon avalanche photodiode (SPAD) with its small active area serving as a confocal aperture. A vibrational spectrum is acquired in Fourier transform mode with two IR pulses derived from an interferometer.

The quality of the double resonance condition plays a crucial role for achieving sensitive FEIR vibrational detection, demonstrated here with the fluorophore Coumarin 6 (C6) in acetonitrile- d_3 . Figure 1c shows that the tunable IR pulses have the spectral breadth to be resonant with the carbonyl ($\nu_{\text{C=O}}$) and three highest frequency C=C ring ($\nu_{\text{R1-3}}$) vibrations when centered at $\omega_{\text{IR}} = 1620 \text{ cm}^{-1}$. Figure 1d shows the electronic absorption and fluorescence spectra of C6. Maximal resonance for the encoding transition is achieved when the sum of IR and visible center frequencies ($\omega_{\text{IR}} + \omega_{\text{vis}} = 20980$

cm^{-1} , $\lambda_{\text{sum}} = 477 \text{ nm}$) falls near the peak of the electronic absorption band. However, the visible pulse (fixed center frequency $\omega_{\text{vis}} = 19360 \text{ cm}^{-1}$, $\lambda_{\text{vis}} = 517 \text{ nm}$) alone directly excites the red tail of the band, creating undesirable background fluorescence. The resonance condition shown in Figure 1d is likely a nearly ideal compromise between large FEIR resonance and low one-photon background, but could be further optimized with a tunable visible pulse.

Figure 1e shows the total fluorescence count rate from a $30 \mu\text{M}$ C6 solution as a function of the IR-visible pulse time delay, or encoding delay τ_{enc} , for excitation with a single IR pulse. The baseline apparent for $\tau_{\text{enc}} < 0$ is the sum of the aforementioned one-photon excited fluorescence F_0 and nonmolecular background B , including solvent Raman scattering, impurity and optics fluorescence, and detector dark counts. After a nearly pulse-limited rise to a maximum labeled F_1 , the FEIR signal decays away, tracking the vibrations' population relaxation kinetics. The FEIR vibrational spectrum at $\tau_{\text{enc}} = 600 \text{ fs}$, corresponding to the signal maximum in Figure 1e, is shown in Figure 1f overlaid on the FTIR linear absorption spectrum scaled by the spectrum of the IR pulse. The FEIR spectrum is free of background due to the Fourier transform acquisition modality. Recording FEIR spectra as a function of τ_{enc} would resolve the decay transient by vibrational mode. Differences in relative peak amplitudes between the FEIR and conventional IR spectra are due to the contribution of vibrational-electronic coupling in the former, which controls the strength of the electronic encoding transition. Specifically, the factor of 5 difference in FEIR intensity between the similarly IR-intense ν_{R2} and ν_{R1} modes at

1586 and 1616 cm^{-1} as well as the nearly absent $\nu_{\text{C}=\text{O}}$ band at 1712 cm^{-1} is well described by these vibrations' respective Huang–Rhys factors.²⁴

The ultimate detection sensitivity of an FEIR measurement hinges upon the ability to resolve the FEIR signal F_1 against the background $F_0 + B$, quantified by the modulation ratio $M = F_1/(F_0 + B)$. Maximizing M therefore requires simultaneously optimizing the brightness of molecular fluorescence $F_1 + F_0$ against B , as well as F_1 against F_0 —a nontrivial problem strongly influenced by the double resonance condition discussed above.

Figure 2a shows the concentration dependence of the maximum F_1 signal and background level $F_0 + B$ for C6, scaled

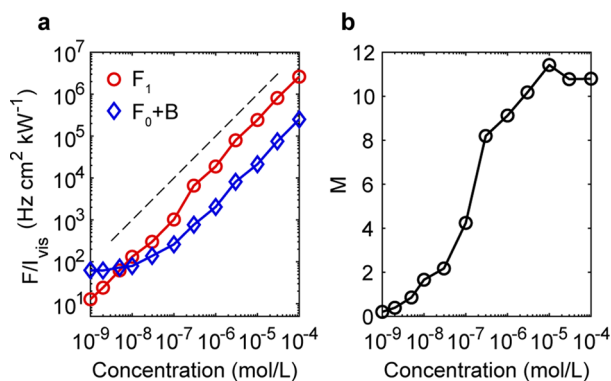


Figure 2. (a) C6 concentration dependence of F_1/I_{vis} (red circles) and $(F_0 + B)/I_{\text{vis}}$ (blue diamonds). Dashed line shows a linear dependence for reference. (b) Modulation ratios M corresponding to panel (a).

by the visible excitation intensity I_{vis} . While the FEIR signal is roughly linear in concentration across the entire range, the

background levels off to a concentration-independent value in the nM regime. This constant level represents I_{vis} -dependent contributions to B , likely solvent Raman scattering or fluorescence from impurities and optics. Correspondingly, M (Figure 2b) falls by nearly 2 orders of magnitude from its B -free value of ~ 11 in the μM range. Using time-correlated single-photon counting (TCSPC), prompt scattering background can be suppressed by time-gating data acquisition for photon arrivals between 1 and 15 ns after the encoding pulse (Supporting Information Section 3). At the lowest 1 nM concentration investigated, this results in a 4-fold reduction in background at the expense of 30% loss in FEIR signal, improving M from 0.2 to 0.6.

As a demonstration of SM sensitivity, we perform fluctuation correlation spectroscopy with the FEIR signal to count the average number of molecules that contribute at a given time. In analogy to FCS,²⁵ we measure the correlation function $G(t) = \langle \delta F(0)\delta F(t) \rangle / \langle F \rangle^2$, where $F(t)$ is the real-time photon stream from an FEIR measurement with optical delays fixed at the maximum signal level ($\tau_{\text{IR}} = 0$ fs, $\tau_{\text{enc}} = 600$ fs for C6). Like a conventional FCS experiment, diffusion of molecules through the probe volume produces spontaneous fluctuations in $F(t)$, causing $G(t)$ to decay with the characteristic time scale of these transits with early time amplitude given by the inverse of the average molecule number $G(0) = \langle N \rangle^{-1}$.

Figure 3a shows FEIR correlation functions from C6 solutions at 1, 2, 5, and 10 nM along with fits to a standard diffusion model assuming a 3D-ellipsoidal Gaussian probe volume (Supporting Information Section 5). As demonstrated in Figure 3b, $\langle N \rangle$ extracted from the fits depends linearly on concentration, with roughly one molecule at 1 nM. The dependence of $G(0)$ on the starting edge of the time gate used for the 1 nM correlation function reaches ~ 1.5 for gates > 2 ns (Figure S4), and we take the corresponding value of $\langle N \rangle = 0.65$ as our estimate of the average molecule number. The F_1

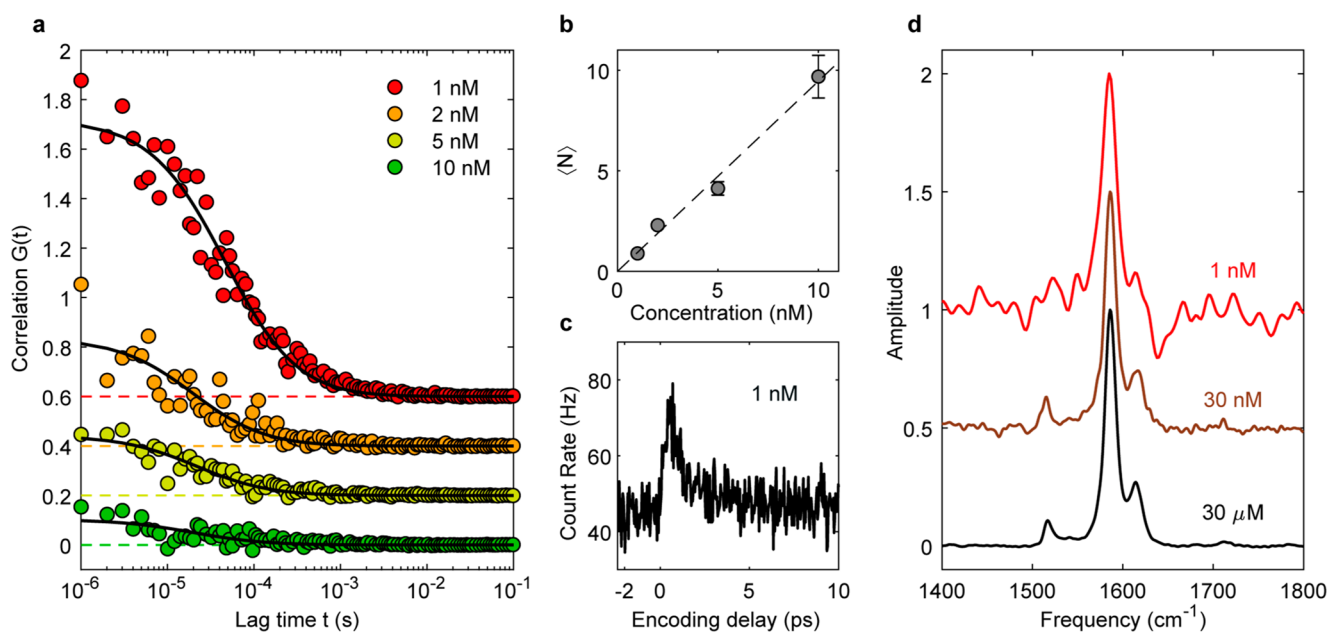


Figure 3. (a) FEIR correlation functions from C6 solutions at 1, 2, 5, and 10 nM (offset for clarity with zero levels indicated by dashed lines). Fits are shown by black lines. (b) $\langle N \rangle = G(0)^{-1}$ from the fits in (a) as a function of concentration, with the linear trend shown by a dashed line. (c) 1-IR-pulse FEIR transient from the 1 nM solution. (d) FEIR spectra at 1 nM, 30 nM, and 30 μM (offset for clarity). The visible pulse energy was 25 pJ for (a), (b), and the 1 nM spectrum in (d), and 12 pJ in (c). Acquisition times were 60 min in (a), and 30 min for (c) and 1 and 30 nM data in (d).

count rate per molecule (ungated) is 110 Hz, which, accounting for the 0.63 fluorescence quantum yield and estimated 1% instrument collection efficiency, corresponds to a 2% overall excitation efficiency per pulse sequence.²⁶ Figure 3c and 3d show the FEIR decay transient and spectrum recorded from the 1 nM solution, demonstrating that the vibrational relaxation and frequency of the brightest ring mode ν_{R2} can still be reliably measured at this level.

We note that the FEIR experiments shown here are fundamentally ensemble measurements, even if $\langle N \rangle < 1$. To clarify this point we highlight the distinction, commonly invoked in the context of FCS within SM fluorescence,²⁷ between SM detection—exclusively observing a particular individual for an extended period—and SM sensitivity—the ability to measure signals and resolve changes caused by individuals. Our proof-of-principle demonstration of FEIR correlation spectroscopy (FEIR-CS) establishes SM sensitivity in that it requires the observation of correlated bursts of FEIR photons from individual molecules. Furthermore, our determination that ensemble FEIR vibrational spectra and relaxation transients can be measured “one molecule at a time” is an encouraging sensitivity milestone along the path toward realizing true SM observation. Many opportunities to optimize this technique are available, including tunable visible excitation, increasing collection efficiency, and—crucially—higher repetition rates, and we note that the pros and cons established by comparison to the related SM SREF spectroscopy developed by Min and co-workers—featuring tunable, frequency-domain stimulated Raman excitation—will offer important insight.^{18,19,28}

As an intermediate step toward SM spectroscopy, FEIR-CS has potential as a powerful vibrational probe of chemical processes in solution, just as FCS often plays an auxiliary role to SM fluorescence experiments. While vibrational analogues of FCS using Raman scattering have been implemented previously, to our knowledge FEIR-CS is the first to be sensitive enough for use with single molecules.^{29–31} Changes in vibrational frequencies due to chemical interconversion or specific molecular interactions in an equilibrium state could be sensed as FEIR signal fluctuations and monitored via the correlation function. Fourier transform excitation with the IR pulse pair suggests the possibility of more sophisticated frequency-resolved FEIR-CS experiments, similar in concept to photon correlation Fourier spectroscopy,^{32,33} which could track microsecond spectral diffusion processes.

In conclusion, we have demonstrated that FEIR vibrational spectroscopy can be performed with SM sensitivity. Careful optimization of the resonance condition is crucial for achieving sufficient signal brightness, while time-resolved photon detection can significantly reduce background levels. We demonstrated proof-of-concept FEIR-CS, which has the potential for development as a vibrational analogue of FCS for studying kinetics of chemical systems in solution with enhanced structural sensitivity. With improvements to the methods reported here, we believe true SM vibrational detection using FEIR spectroscopy is within reach.

■ ASSOCIATED CONTENT

SI Supporting Information

The Supporting Information is available free of charge at <https://pubs.acs.org/doi/10.1021/jacs.1c00542>.

Experimental methods and further details of data acquisition and processing (PDF)

■ AUTHOR INFORMATION

Corresponding Author

Andrei Tokmakoff – Department of Chemistry, James Franck Institute, and Institute for Biophysical Dynamics, The University of Chicago, Chicago, Illinois 60637, United States; orcid.org/0000-0002-2434-8744; Email: tokmakoff@uchicago.edu

Authors

Lukas Whaley-Mayda – Department of Chemistry, James Franck Institute, and Institute for Biophysical Dynamics, The University of Chicago, Chicago, Illinois 60637, United States

Abhirup Guha – Department of Chemistry, James Franck Institute, and Institute for Biophysical Dynamics, The University of Chicago, Chicago, Illinois 60637, United States

Samuel B. Penwell – Department of Chemistry, James Franck Institute, and Institute for Biophysical Dynamics, The University of Chicago, Chicago, Illinois 60637, United States

Complete contact information is available at: <https://pubs.acs.org/10.1021/jacs.1c00542>

Notes

The authors declare no competing financial interest.

■ ACKNOWLEDGMENTS

This work was supported by a grant from the National Science Foundation (CHE-1856684).

■ REFERENCES

- (1) Moerner, W. E.; Kador, L. Optical detection and spectroscopy of single molecules in a solid. *Phys. Rev. Lett.* **1989**, *62*, 2535–2538.
- (2) Orrit, M.; Bernard, J. Single pentacene molecules detected by fluorescence excitation in a p-terphenyl crystal. *Phys. Rev. Lett.* **1990**, *65*, 2716–2719.
- (3) Ambrose, W. P.; Moerner, W. E. Fluorescence spectroscopy and spectral diffusion of single impurity molecules in a crystal. *Nature* **1991**, *349*, 225–227.
- (4) Xie, X. S.; Dunn, R. C. Probing single molecule dynamics. *Science* **1994**, *265*, 361–364.
- (5) Moerner, W. E.; Shechtman, Y.; Wang, Q. Single-molecule spectroscopy and imaging over the decades. *Faraday Discuss.* **2015**, *184*, 9–36.
- (6) Kneipp, K.; Wang, Y.; Kneipp, H.; Perelman, L. T.; Itzkan, I.; Dasari, R. R.; Feld, M. S. Single molecule detection using surface-enhanced raman scattering (SERS). *Phys. Rev. Lett.* **1997**, *78*, 1667–1670.
- (7) Haran, G. Single-molecule raman spectroscopy: A probe of surface dynamics and plasmonic fields. *Acc. Chem. Res.* **2010**, *43*, 1135–1143.
- (8) Dey, S.; Apkarian, V. A.; Potma, E. O.; Fishman, D. A.; Banik, M.; Yampolsky, S.; Hulkko, E. Seeing a Single Molecule Vibrate through Time-Resolved Coherent Anti-Stokes Raman Scattering. *Nat. Photonics* **2014**, *8*, 650–656.
- (9) Zrimsek, A. B.; Chiang, N.; Mattei, M.; Zaleski, S.; McAnally, M. O.; Chapman, C. T.; Henry, A. I.; Schatz, G. C.; Van Duyne, R. P. Single-Molecule Chemistry with Surface- and Tip-Enhanced Raman Spectroscopy. *Chem. Rev.* **2017**, *117*, 7583–7613.
- (10) Ruggeri, F. S.; Mannini, B.; Schmid, R.; Vendruscolo, M.; Knowles, T. P. J. Single molecule secondary structure determination of proteins through infrared absorption nanospectroscopy. *Nat. Commun.* **2020**, *11*, 1–9.

- (11) Xu, X. G.; Rang, M.; Craig, I. M.; Raschke, M. B. Pushing the sample-size limit of infrared vibrational nanospectroscopy: From monolayer toward single molecule sensitivity. *J. Phys. Chem. Lett.* **2012**, *3*, 1836–1841.
- (12) Stipe, B. C.; Rezaei, M. A.; Ho, W. Single-molecule vibrational spectroscopy and microscopy. *Science* **1998**, *280*, 1732–1735.
- (13) Laubereau, A.; Seilmeier, A.; Kaiser, W. A New Technique to Measure Ultrashort Vibrational Relaxation Times in Liquid Systems. *Chem. Phys. Lett.* **1975**, *36*, 232–237.
- (14) Wright, J. C. Double Resonance Excitation of Fluorescence in the Condensed Phase—An Alternative to Infrared, Raman, and Fluorescence Spectroscopy. *Appl. Spectrosc.* **1980**, *34*, 151–157.
- (15) Lee, S. H.; Nguyen, D. C.; Wright, J. C. Double Resonance Excitation of Fluorescence by Stimulated Raman Scattering. *Appl. Spectrosc.* **1983**, *37* (5), 472–474.
- (16) Hübner, H. J.; Wörner, M.; Kaiser, W.; Seilmeier, A. Subpicosecond vibrational relaxation of skeletal modes in polyatomic molecules. *Chem. Phys. Lett.* **1991**, *182*, 315–320.
- (17) Winterhalder, M. J.; Zumbusch, a.; Lippitz, M.; Orrit, M. Toward far-field vibrational spectroscopy of single molecules at room temperature. *J. Phys. Chem. B* **2011**, *115*, 5425–30.
- (18) Xiong, H.; Min, W. Combining the best of two worlds: Stimulated Raman excited fluorescence. *J. Chem. Phys.* **2020**, *153*, 210901–210901.
- (19) Xiong, H.; Shi, L.; Wei, L.; Shen, Y.; Long, R.; Zhao, Z.; Min, W. Stimulated Raman excited fluorescence spectroscopy and imaging. *Nat. Photonics* **2019**, *13*, 412–417.
- (20) Mastron, J. N.; Tokmakoff, A. Two-Photon-Excited Fluorescence-Encoded Infrared Spectroscopy. *J. Phys. Chem. A* **2016**, *120*, 9178–9187.
- (21) Mastron, J. N.; Tokmakoff, A. Fourier Transform Fluorescence-Encoded Infrared Spectroscopy. *J. Phys. Chem. A* **2018**, *122*, 554–562.
- (22) Whaley-Mayda, L.; Penwell, S. B.; Tokmakoff, A. Fluorescence-Encoded Infrared Spectroscopy: Ultrafast Vibrational Spectroscopy on Small Ensembles of Molecules in Solution. *J. Phys. Chem. Lett.* **2019**, *10*, 1967–1972.
- (23) Penwell, S. B.; Whaley-Mayda, L.; Tokmakoff, A. Single-stage MHz mid-IR OPA using LiGaS₂ and a fiber laser pump source. *Opt. Lett.* **2018**, *43*, 1363–1363.
- (24) Von Cosel, J.; Cerezo, J.; Kern-Michler, D.; Neumann, C.; Van Wilderen, L. J. G. W.; Bredenbeck, J.; Santoro, F.; Burghardt, I. Vibrationally resolved electronic spectra including vibrational pre-excitation: Theory and application to VIPER spectroscopy. *J. Chem. Phys.* **2017**, *147*.
- (25) Krichevsky, O.; Bonnet, G. Fluorescence correlation spectroscopy: the technique and its applications. *Rep. Prog. Phys.* **2002**, *65*, 251–297.
- (26) Jones, G.; Jackson, W. R.; Choi, C. Y.; Bergmark, W. R. Solvent effects on emission yield and lifetime for coumarin laser dyes. Requirements for a rotatory decay mechanism. *J. Phys. Chem.* **1985**, *89*, 294–300.
- (27) Moerner, W. E.; Fromm, D. P. Methods of single-molecule fluorescence spectroscopy and microscopy. *Rev. Sci. Instrum.* **2003**, *74*, 3597–3619.
- (28) Xiong, H.; Qian, N.; Miao, Y.; Zhao, Z.; Min, W. Stimulated Raman Excited Fluorescence Spectroscopy of Visible Dyes. *J. Phys. Chem. Lett.* **2019**, *10*, 3563–3570.
- (29) Schrof, W.; Klingler, J.; Rozouvan, S.; Horn, D. Raman correlation spectroscopy: A method for studying chemical composition and dynamics of disperse systems. *Phys. Rev. E: Stat. Phys., Plasmas, Fluids, Relat. Interdiscip. Top.* **1998**, *57*, R2523–R2526.
- (30) Cheng, J.; Potma, E. O.; Xie, X. S. Coherent Anti-Stokes Raman Scattering Correlation Spectroscopy: Probing Dynamical Processes with Chemical Selectivity. *J. Phys. Chem. A* **2002**, *106*, 8561–8568.
- (31) Barbara, A.; Dubois, F.; Quémerais, P.; Eng, L. Non-resonant and non-enhanced Raman Correlation Spectroscopy. *Opt. Express* **2013**, *21*, 15418–15418.
- (32) Brokmann, X.; Bawendi, M.; Coolen, L.; Hermier, J.-P. Photon-correlation Fourier spectroscopy. *Opt. Express* **2006**, *14*, 6333–6333.
- (33) Marshall, L. F.; Cui, J.; Brokmann, X.; Bawendi, M. G. Extracting spectral dynamics from single chromophores in solution. *Phys. Rev. Lett.* **2010**, *105*, 1–4.